Towards Multi-Sensor Equivariant Filter Design

Martin Scheiber[1], Alessandro Fornasier[1], Christian Brommer[1], and Stephan Weiss[1]

***Abstract*—Equivariant filters (EqFs) are on the rise for robotic localization applications. In its design derived from the extended Kalman filter (EKF), the EqF provides many advantageous properties, though they grow in design complexity with multiple sensors. Each state added to the filter necessitates new derivations for corresponding symmetries and group actions. This paper presents a basic setup – the building blocks – for future equivariant filter design. We outline the symmetries and group actions for all possible rigid-body calibration states (rotational, translational, and pose) and states for direction vectors and height sensor biases. These fundamental components enable equivariant multi-sensor fusion for UAVs equipped with the most common sensors, such as GNSS, magnetometer, pressure sensor, or loosely coupled pose sensors (e.g., vision). Our results demonstrate such a multi-sensor EqF.**

I. Introduction and Related Work

In recent years, a new type of filter-based estimation has emerged: the equivariant filter (EqF). Originally introduced by *van Goor et al.* [1], [2], this filter is an extension of the well-known extended Kalman filter (EKF), which introduces an equivariant symmetry group to perform estimation on. This group change comes with a set of advantageous properties: guaranteed convergence, consistent estimation, and better error linearization, to name just a few. Compared to other state-of-the-art filters like the invariant EKF (IEKF) [3], EqFs can more efficiently include additional states such as bias terms or calibrations on the symmetry group and thus inherit the aforementioned properties for these states as well [4].

Brommer et al. [5] introduced a state-of-the-art truly modular method for EKF-based multi-sensor localization, extending the insights of *Lynen et al.* [6]. To the knowledge of the authors, many more methods for multi-sensor localization exist [7], but do not facilitate modularity. In addition, other filters such as the better performing TF-IEKF by *Baurrau and Bonnabel* [8] do not consider a multitude of additional calibration or sensor states, but rather individual sensor setups [9], [10].

The theory suggests EqFs should be the choice of filter for uncrewed aerial vehicle (UAV) localization [4]. However, their derivation can be quite complex, especially when a multitude of sensors, such as global navigation satellite system (GNSS) sensor, magnetometer, or pressure sensor, are used. Recent examples of equivariant filters for inertial navigation system (INS) provide single and individual derivations for, e.g., attitude estimation [11], (multi) GNSS estimation [12], [13], or tightly-coupled visual-inertial odometry (VIO) [14], [15]. Yet, combining the filter derivation of these separate works is not straightforward.

Therefore, with this paper, we introduce a general guide on equivariant filter design for robotic systems in 3D space. By providing the basic building blocks for core navigation states, rigid-body calibration states, and common UAV sensor modalities, we aim to provide a basis for future, simpler equivariant estimation. The measurement functions and additional states considered for estimation are presented in Table I.

TABLE I
Sensor States and Measurements

Magnetometer	$\boldsymbol{\xi}_M$	$(\mathbf{S}, \mathbf{m}) \in \mathcal{SO}(3) \times \mathbb{R}^3$
	$h_M(\boldsymbol{\xi})$	$({}^G\mathbf{R}_I\mathbf{S})^\mathsf{T}\mathbf{m} \in \mathbb{R}^3 \setminus \{\mathbf{0}_3\}$
Position	$\boldsymbol{\xi}_T$	$\mathbf{t} \in \mathbb{R}^3$
	$h_T(\boldsymbol{\xi})$	${}^G\mathbf{R}_I^\mathsf{T}(\boldsymbol{\pi} - ({}^G\mathbf{p}_I + {}^G\mathbf{R}_I\mathbf{t})) \in \mathbb{R}^3$
Velocity	$\boldsymbol{\xi}_V$	$\mathbf{t} \in \mathbb{R}^3$
	$h_V(\boldsymbol{\xi})$	${}^G\mathbf{R}_I^\mathsf{T}(\boldsymbol{\nu} - ({}^G\mathbf{v}_I + {}^G\mathbf{R}_I\mathbf{t}^{\wedge\, I}\boldsymbol{\omega})) \in \mathbb{R}^3$
Pose	$\boldsymbol{\xi}_P$	$\mathbf{L} \in \mathcal{SE}(3)$
	$h_P(\boldsymbol{\xi})$	$\mathbf{P}\mathbf{L} \in \mathcal{SE}(3)$
Pressure	$\boldsymbol{\xi}_H$	$(\mathbf{t}, h) \in \mathbb{R}^3 \times \mathbb{R}$
	$h_H(\boldsymbol{\xi})$	$\mathbf{e}_z^\mathsf{T}({}^G\mathbf{p}_I + {}^G\mathbf{R}_I\mathbf{t}) + h \in \mathbb{R}$

II. Multi-Sensor Biased INS

This section introduces the biased INS for multi-sensor setups problem using the mathematical expression of our previous works [4], [12], [15]. For additional sources on equivariant filters, symmetry groups, and Lie algebra we refer the interested reader to [1], [16], [17].

A. Core Navigation State

For the equivariant theory and system modeling, it is easier to use the matrix notation of Lie groups (where applicable). Therefore, by considering $\boldsymbol{\xi}_C = (\mathbf{T}, \mathbf{b}) \in {}^C\mathcal{M} := \mathcal{SE}_2(3) \times \mathbb{R}^9$ to be the core state space of the system, with the extended pose $\mathbf{T} = (\mathbf{R}, \mathbf{v}, \mathbf{p}) \in \mathcal{SE}_2(3)$ and biases $\mathbf{b} = (\mathbf{b}_\omega, \mathbf{b}_a, \mathbf{b}_\nu) \in \mathbb{R}^9$, and defining the input $u = (u, \boldsymbol{\tau}) \in \mathbb{L} \subset \mathbb{R}^{18}$, with $u = (\boldsymbol{\omega}, \mathbf{a}, \boldsymbol{\nu}) \subset \mathbb{R}^9$ and $\boldsymbol{\tau} = (\boldsymbol{\tau}_\omega, \boldsymbol{\tau}_a, \boldsymbol{\tau}_\nu) \subset \mathbb{R}^9$, we can write the systems dynamics in the following matrix form

$$\dot{\mathbf{T}} = \mathbf{T}(\mathbf{W} - \mathbf{B} + \mathbf{N}) + (\mathbf{G} - \mathbf{N})\mathbf{T}, \tag{1a}$$

$$\dot{\mathbf{b}} = \boldsymbol{\tau}, \tag{1b}$$

where, $\mathbf{W} = u^\wedge$, and $\mathbf{B} = \mathbf{b}^\wedge$. $\mathbf{G}$ and $\mathbf{N}$ are defined according to [15].

This work has received funding in part from the European Union's Horizon 2020 research and innovation programme under grant agreement 871260, and in part fromthe Austrian Federal Ministry for Climate Action, Environment, Energy, Mobility, Innovation and Technology (BMK) under grant agreement 895156 (NIKE-SwarmNav).

[1]All authors are with the Institute of Smart Systems Technologies, Control of Networked Systems Group, University of Klagenfurt, Klagenfurt, Austria. Email: {firstname.lastname}@ieee.org

B. Sensor Models

1) Magnetometer: A magnetometer measures the magnetic field direction $\mathbf{m} \in \mathbb{R}^3 \setminus \{\mathbf{0}_3\}$ in the sensor frame. Given that the sensor frame might not align with the inertial measurement unit (IMU) frame, an additional calibration state $\mathbf{S} \in \mathcal{SO}(3)$ is introduced to generate the following sensor measurement

$$h_{M}(\boldsymbol{\xi}) = (\mathbf{RS})^{\mathsf{T}}\mathbf{m} = y_M \in {}^{M}\mathcal{N} \subset \mathbb{R}^3. \tag{2}$$

The dynamics for these additional states can in general be defined with the arbitrary inputs $u_{\mathbf{S}} \in {}^{S}\mathbb{L} \subset \mathbb{R}^3$ and $u_{\mathbf{m}} \in {}^{m}\mathbb{L} \subset \mathbb{R}^3$:

$$\dot{\mathbf{S}} = \mathbf{S}u_{\mathbf{S}}^{\wedge}, \qquad \text{and} \qquad \dot{\mathbf{m}} = u_{\mathbf{m}}. \tag{3}$$

2) GNSS: Global navigation satellite system sensors can provide both position and velocity information. They also require a calibration for the translation $\mathbf{t} \in \mathbb{R}^3$ between the sensor frame and the IMU frame. In general, the measurements are modeled as

$$\pi = \mathbf{Rt} + \mathbf{p}, \qquad \text{and} \qquad \tau = \mathbf{v} + \mathbf{Rt}^{\wedge}\boldsymbol{\omega},$$

for position and velocity, respectively. However, these measurement models cannot produce an transitive right output action. Therefore, we reconstruct the measurement function to measure ideally $\mathbf{0}_d$ in a body-centric formulation

$$h_{T}(\boldsymbol{\xi}) = \mathbf{R}^{\mathsf{T}}\big(\pi - (\mathbf{p} + \mathbf{Rt})\big) = y_T \in {}^{T}\mathcal{N} \subset \mathbb{R}^3, \tag{4}$$

$$h_{V}(\boldsymbol{\xi}) = \mathbf{R}^{\mathsf{T}}\big(\tau - (\mathbf{v} + \mathbf{Rt}^{\wedge}\boldsymbol{\omega})\big) = y_V \in {}^{V}\mathcal{N} \subset \mathbb{R}^3. \tag{5}$$

Similar to the rotational calibration, if it is added as a state, the dynamics for the translational calibration are

$$\dot{\mathbf{t}} = u_{\mathbf{t}}, \tag{6}$$

with $u_{\mathbf{t}} \in {}^{t}\mathbb{L} \subset \mathbb{R}^3$.

3) Pose Sensor: Pose sensors measure the 6-DoF pose of a vehicle within a navigation frame. For this work, we consider that this navigation frame coincides with the global frame through a static, known calibration. Additionally, a pose sensor can have an rigid body calibration $\mathbf{L} := \big(\mathbf{L}_R, \mathbf{L}_p\big) \in \mathcal{SE}(3)$ between the sensor frame and IMU frame. The measurement function and eventual dynamics are then

$$h_{P}(\boldsymbol{\xi}) = \mathbf{PL} = y_P \in {}^{P}\mathcal{N} \subset \mathbb{R}^{4\times4}, \tag{7}$$

$$\dot{\mathbf{L}} = \mathbf{L}u_{\mathbf{L}}^{\wedge}, \tag{8}$$

where $\mathbf{P}$ is the $\mathcal{SE}(3)$ pose of $\mathbf{T}$, i.e. $\mathbf{P} = \theta(\mathbf{T})$, and $u_{\mathbf{L}} \in {}^{L}\mathbb{L} \subset \mathbb{R}^6$ is an arbitrary input.

4) Pressure Sensor: Generally pressure sensor models depend on the medium they are used in, for robotics either barometric or liquid pressure. To simplify the usage of this sensor for any robotic platform, within this letter we consider the pressure sensor as a 1D height sensor with respect to a specific reference frame (typically sea level). However, the sea level rarely coincides with the z-origin of the global navigation frame, and therefore an additional "bias" term $h \in \mathbb{R}$ needs to be added to the state. Further, $\mathbf{t} \in \mathbb{R}^3$ represents the calibration between the sensor and the IMU, and $\mathbf{e}_z \in \mathbb{R}^3$ is the unit vector in z-direction,

$$h_{H}(\boldsymbol{\xi}) = \mathbf{e}_z^{\mathsf{T}}(\mathbf{p} + \mathbf{Rt}) + h = y_H \in {}^{H}\mathcal{N} \subset \mathbb{R}. \tag{9}$$

III. State Symmetries

In multi-sensor equivariant filter design, it is desirable to find state-independent symmetry groups to allow modular sensor suits. Indeed, it is possible to define all additional symmetries and group actions independently of each other, with the exception of the core state symmetry. However, this does not introduce any problems, as the core state needs to be tracked anyway, regardless of the sensor type. Therefore, we first present the biased-INS symmetry and then the derived, individual state symmetries, based on the states introduced in the section above.

A. Core Navigation State Symmetry

Let the symmetry group of the core state be the tangent group as defined in [4], ${}^{C}\mathbf{G} := \mathbf{SE}_2(3) \ltimes \mathfrak{se}_2(3)$. Let $X_C = (D, \delta) \in {}^{C}\mathbf{G}$ be an element of the symmetry group, with $D = (A, a, b) \in \mathbf{SE}_2(3)$. The inverse element is given by $X^{\text{-}1} = \big(D^{\text{-}1}, \text{-}\operatorname{Ad}_{D^{\text{-}1}}[\delta]\big)$ with $D^{\text{-}1} = (A^{\mathsf{T}}, \text{-}A^{\mathsf{T}}a, \text{-}A^{\mathsf{T}}b)$, and the identity element of $\mathbf{G}$ is $\mathrm{id} = \big((\mathbf{I}_3, \mathbf{0}_{3\times1}, \mathbf{0}_{3\times1}), \mathbf{0}_{9\times1}^{\wedge}\big) \in {}^{C}\mathbf{G}$.

Lemma 3.1. *The right state group action of ${}^{C}\mathbf{G}$ on ${}^{C}\mathcal{M}$, $\phi : {}^{C}\mathbf{G} \times {}^{C}\mathcal{M} \to {}^{C}\mathcal{M}$ and the right input group action of ${}^{C}\mathbf{G}$ on ${}^{C}\mathbb{L}$, $\psi : {}^{C}\mathbf{G} \times {}^{C}\mathbb{L} \to {}^{C}\mathbb{L}$, are defined as*

$${}^{C}\phi(X, \boldsymbol{\xi}) := \Big(\mathbf{T}D, \mathbf{Ad}_{D^{\text{-}1}}^{\vee}(\mathbf{b} - \delta)\Big), \tag{10a}$$

$${}^{C}\psi(X, u) := \Big(\mathbf{Ad}_{D^{\text{-}1}}^{\vee}(u_{\mathbf{T}} - \delta) + \Omega(D), \mathbf{Ad}_{D^{\text{-}1}}^{\vee}(u_{\mathbf{b}})\Big), \tag{10b}$$

with $\Omega(D)$ as defined in [4].

To lift the dynamics of (1) onto the symmetry a system lift is further required:

Lemma 3.2. *The lift $\Lambda : {}^{C}\mathcal{M} \times {}^{C}\mathbb{L} \to {}^{C}\mathbf{G}$ is defined as*

$${}^{C}\Lambda_{D}(\boldsymbol{\xi}, u) = \mathbf{T}(\mathbf{W} - \mathbf{B} + \mathbf{N}) + \mathbf{T}^{\text{-}1}(\mathbf{G} - \mathbf{N})\mathbf{T}, \tag{11a}$$

$${}^{C}\Lambda_{\delta}(\boldsymbol{\xi}, u) = \mathbf{ad}_{\mathbf{b}}^{\vee}(\Lambda_{D}(\boldsymbol{\xi}, u)) - u_{\mathbf{b}}, \tag{11b}$$

where Λ_D and Λ_δ refer to the lifted elements for D and δ of X_C, respectively.

In what follows we will briefly introduce the symmetry groups, actions, and lifts for the three types of calibration states, rotational, translational, and pose. A summary for these states is presented in Table II.

B. Calibration State Symmetries

Given $\mathbf{S}$, $\mathbf{t}$, and $\mathbf{L}$ for the rotational, translational, and pose calibration, the corresponding symmetry elements can be defined as $E \in \mathbf{SO}(3)$, $\epsilon \in \mathbb{R}^3$, and $F \in \mathbf{SE}(3)$. The properties of the symmetry elements are presented in Table II.

TABLE II
ADDITIONAL SENSOR STATES

STATE	State $\boldsymbol{\xi} \in \mathcal{M}$	Input $\in \mathbb{L}$	Dynamics $\frac{\mathrm{d}\boldsymbol{\xi}}{\mathrm{d}t}$	Symmetry Group $\mathbf{G}$	SG Element X	Inverse X^{-1}	Multiplication XY
Rotational	$\mathbf{S} \in \mathcal{SO}(3)$	$u_{\mathbf{S}} \subset \mathbb{R}^3$	$\mathbf{S}u_{\mathbf{S}}^{\wedge}$	${}^{C}\mathbf{G} \times \mathbf{SO}(3)$	E	E^{T}	$E_X E_Y$
Translational	$\mathbf{t} \in \mathbb{R}^3$	$u_{\mathbf{t}} \subset \mathbb{R}^3$	$u_{\mathbf{t}}$	${}^{C}\mathbf{G} \ltimes \mathbb{R}^3$	ϵ	$-A^{\mathsf{T}}\epsilon$	$A_X\epsilon_Y + \epsilon_X$
Pose	$\mathbf{L} \in \mathcal{SE}(3)$	$u_{\mathbf{L}} \subset \mathbb{R}^6$	$\mathbf{L}u_{\mathbf{L}}^{\wedge}$	${}^{C}\mathbf{G} \times \mathbf{SE}(3)$	F	F^{-1}	$F_X F_Y$
Direction	$\mathbf{m} \in \mathbb{R}^3 \setminus \{\mathbf{0}_3\}$	$u_{\mathbf{m}} \subset \mathbb{R}^3$	$u_{\mathbf{m}}$	${}^{C}\mathbf{G} \times \mathbf{SOT}(3)$	Q	Q^{-1}	$Q_X Q_Y$
Height Bias	$h \in \mathbb{R}$	$u_h \subset \mathbb{R}$	u_h	${}^{C}\mathbf{G} \times \mathbb{R}$	k	$-k$	$k_X + k_Y$

Lemma 3.3. *The symmetry group actions ${}^{i}\phi : {}^{i}\mathbf{G} \times {}^{i}\mathcal{M} \to {}^{i}\mathcal{M}$ for the rotational, translational and pose calibration states are defined as*

$$ {}^{r}\phi\left(X, \boldsymbol{\xi}\right) := A^{\mathsf{T}}\mathbf{S}E, \tag{12} $$
$$ {}^{t}\phi\left(X, \boldsymbol{\xi}\right) := A^{\mathsf{T}}(\mathbf{t} - \epsilon), \tag{13} $$
$$ {}^{p}\phi\left(X, \boldsymbol{\xi}\right) := C^{-1}\mathbf{L}F, \tag{14} $$

respectively. $C := \theta\left(D\right) = (A, b) \in \mathbf{SE}(3)$ is the pose of the core symmetry element.

Lemma 3.4. *The input actions ${}^{i}\psi : {}^{i}\mathbf{G} \times {}^{i}\mathbb{L} \to {}^{i}\mathbb{L}$ for the rotational, translational, and pose calibration states are defined as*

$$ {}^{r}\psi\left(X, u\right) := \mathbf{Ad}^{\vee}_{E^{\mathsf{T}}}(u_{\mathbf{S}}), \tag{15} $$
$$ {}^{t}\psi\left(X, u\right) := A^{\mathsf{T}}u_{\mathbf{t}}, \tag{16} $$
$$ {}^{p}\psi\left(X, u\right) := \mathbf{Ad}^{\vee}_{F^{-1}}(u_{\mathbf{L}}). \tag{17} $$

Lemma 3.5. *The lifts ${}^{i}\Lambda : {}^{i}\mathcal{M} \times {}^{i}\mathbb{L} \to {}^{i}\mathbf{G}$ for the rotational, translational, and pose calibration states are defined as*

$$ {}^{r}\Lambda_{E}\left(\boldsymbol{\xi}, u\right) := \mathbf{S}^{\mathsf{T}}(\boldsymbol{\omega} - \mathbf{b}_{\omega})^{\wedge}\mathbf{S} + u_{\mathbf{S}}^{\wedge}, \tag{18} $$
$$ {}^{t}\Lambda_{\epsilon}\left(\boldsymbol{\xi}, u\right) := \mathbf{t}^{\wedge}(\boldsymbol{\omega} - \mathbf{b}_{\omega}) - u_{\mathbf{t}}, \tag{19} $$
$$ {}^{p}\Lambda_{F}\left(\boldsymbol{\xi}, u\right) := \left(\mathbf{Ad}^{\vee}_{\mathbf{L}^{-1}}(\theta\left({}^{\mathbf{T}}\Lambda\left(\boldsymbol{\xi}, u\right)\right)) + u_{\mathbf{L}}\right)^{\wedge}. \tag{20} $$

The proof for these actions and lift follows our previous works [12], [15], [18].

C. Additional Sensor Symmetries

1) Magnetometer: Given that the magnetic world vector $\mathbf{m}$ is observable [19], an additional symmetry element $Q := \left(R_Q, c_Q\right) \in \mathbf{SOT}(3)$ for the magnetic vector can be added, using the $\mathbf{SOT}(3)$ group [14]. Further, we assume a calibration state $\mathbf{S}$ and symmetry element E to be present.

Lemma 3.6. *The group action, input action, lift, and configuration output for the magnetometer's additional states are defined as*

$$ {}^{m}\phi\left(X, \boldsymbol{\xi}\right) := \mathbf{RS}EQ^{-1}(\mathbf{RS})^{\mathsf{T}}\mathbf{m}, \tag{21} $$
$$ {}^{m}\psi\left(X, u\right) := EQ^{-1}, \tag{22} $$
$$ {}^{m}\Lambda_{R_Q}\left(\boldsymbol{\xi}, u\right) := {}^{r}\Lambda_{E}\left(\boldsymbol{\xi}, u\right) - \frac{(\mathbf{RS})^{\mathsf{T}}(\mathbf{m}^{\wedge}u_{\mathbf{m}})}{\|\mathbf{m}\|^2}, \tag{23a} $$
$$ {}^{m}\Lambda_{c_Q}\left(\boldsymbol{\xi}, u\right) := \frac{\mathbf{m}^{\mathsf{T}}u_{\mathbf{m}}}{\|\mathbf{m}\|^2}, \tag{23b} $$
$$ {}^{M}\rho\left(X, y\right) := Q^{-1}y. \tag{24} $$

2) Pressure: Similar to the direction sensor, the reference offset h of the pressure sensor can be added as a state with the corresponding symmetry element $k \in \mathbb{R}$.

Lemma 3.7. *The group action ${}^{h}\phi$, input action ${}^{h}\psi$, and lift ${}^{h}\Lambda$ for the pressure sensor's additional states are defined as*

$$ {}^{h}\phi\left(X, \boldsymbol{\xi}\right) := h + k, \tag{25} $$
$$ {}^{h}\psi\left(X, u\right) := u_h, \tag{26} $$
$$ {}^{h}\Lambda\left(\boldsymbol{\xi}, u\right) := u_h. \tag{27} $$

While this symmetry does provide input equivariance, no right equivariant output action can be found. While there exist other symmetries that can provide an equivariant output action, they come at the cost of input equivariance. In practice, this results in the propagation step being non-equivariant and thus requires a different derivation for the below presented filter equations. However, since the update is sensor-wise decoupled, having a different derivation for this sensor's update step does not require a different derivation for the other sensors, and thus is favorable to have in multi-sensor scenarios.

3) Position, Velocity, and Pose Sensor: Apart from the calibration, these sensors do not introduce any additional state.

Lemma 3.8. *The configuration outputs ${}^{i}\rho : {}^{h}\mathcal{N} \to {}^{h}\mathcal{N}$ for the position, velocity, and pose sensor are defined as*

$$ {}^{T}\rho\left(X, y\right) := A^{\mathsf{T}}(y_T - b + \epsilon), \tag{28} $$
$$ {}^{V}\rho\left(X, y, u\right) := A^{\mathsf{T}}(y_V - a + \boldsymbol{\omega}^{\wedge}\epsilon), \tag{29} $$
$$ {}^{P}\rho\left(X, y\right) := y_P F. \tag{30} $$

IV. EQUIVARIANT FILTER DESIGN

The equivariant filter is based on the EKF in its design [1]. Let $\hat{X}_k \in \mathbf{G}$ be the estimate on the symmetry group at time t_k, and $\boldsymbol{\Sigma}_k \subset \mathbb{R}^{n \times n}$ be its covariance matrix, with $n = \dim \mathbf{G}$. We make the choice of using normal coordinates as local coordinates ε for the global equivariant error $e := \phi_{\hat{X}^{-1}}\left(\boldsymbol{\xi}\right)$, hence

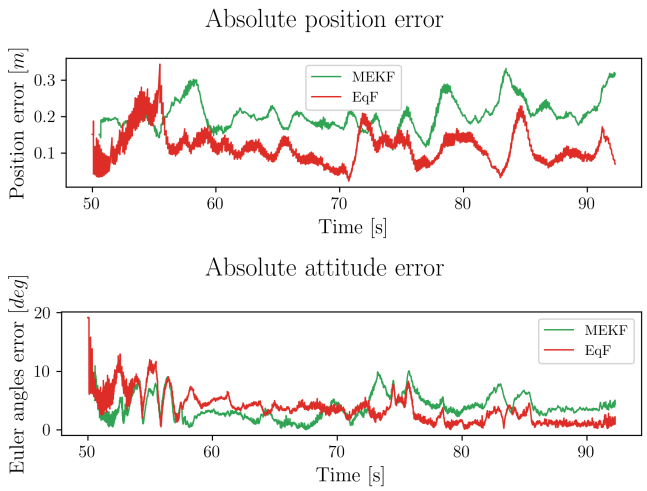

Fig. 1. Error plots for the position and attitude results for the *Mars 5* trajectory from the *Insane* dataset, comparing the performance of our EqF (red) and the MEKF of [5] (green).

$\varepsilon = \vartheta(e) := \log_{\mathbf{G}}(\phi_{\boldsymbol{\xi}}^{-1}(e))^{\vee} \in \mathbb{R}^n$ with $\log_{\mathbf{G}} : \mathbf{G} \to \mathfrak{g}$ being the logarithm of the symmetry group. Then the error dynamics can be defined as

$$\mathrm{d}\varepsilon = \mathbf{A}_t^0 \varepsilon \mathrm{d}t + \mathbf{B}_t \mathrm{d}\mu_u, \tag{31a}$$

$$\mathrm{d}\widetilde{y} = \mathbf{C}_t^{\star} \varepsilon \mathrm{d}t. \tag{31b}$$

In full equivariant systems the matrices can be derived with [17]. The filter implementation then extends [13] with the additional sensor modalities and updates.

V. Results

We implemented the presented EqF[1] with each of the sensor modalities as shown in Table I being used once. Our filter is then tested using the *Insane* dataset [20], as it provides all presented sensors on various different UAV flights.

In Fig. 1 the position and attitude error is displayed using the provided ground truth of the dataset. As the EqF is initialized with the core states set to identity the attitude experiences a slightly longer transient phase. We compare it to the truly-modular multiplicative EKF (MEKF) *MaRS* [5], which has the same states and estimates enabled as the EqF.

Additionally, the auxiliary state estimates for two GNSS sensors, a magnetometer, and a pressure sensor are displayed in Fig. 2. As can be seen, the calibration states converge rather fast. Further, the magnetic world vector is estimated correctly, while the pressure bias can handle the noisy and drift-effected measurements of the pressure sensor.

VI. Conclusion

With this paper we presented the building blocks of an equivariant filter for UAV localization using various sensor modalities. We introduced additional tracking states, symmetry group actions, and dynamics lifts required for such a filter and showed it's performance using the *Insane* dataset.

[1]Source code will be made available on GitHub with full paper publication.

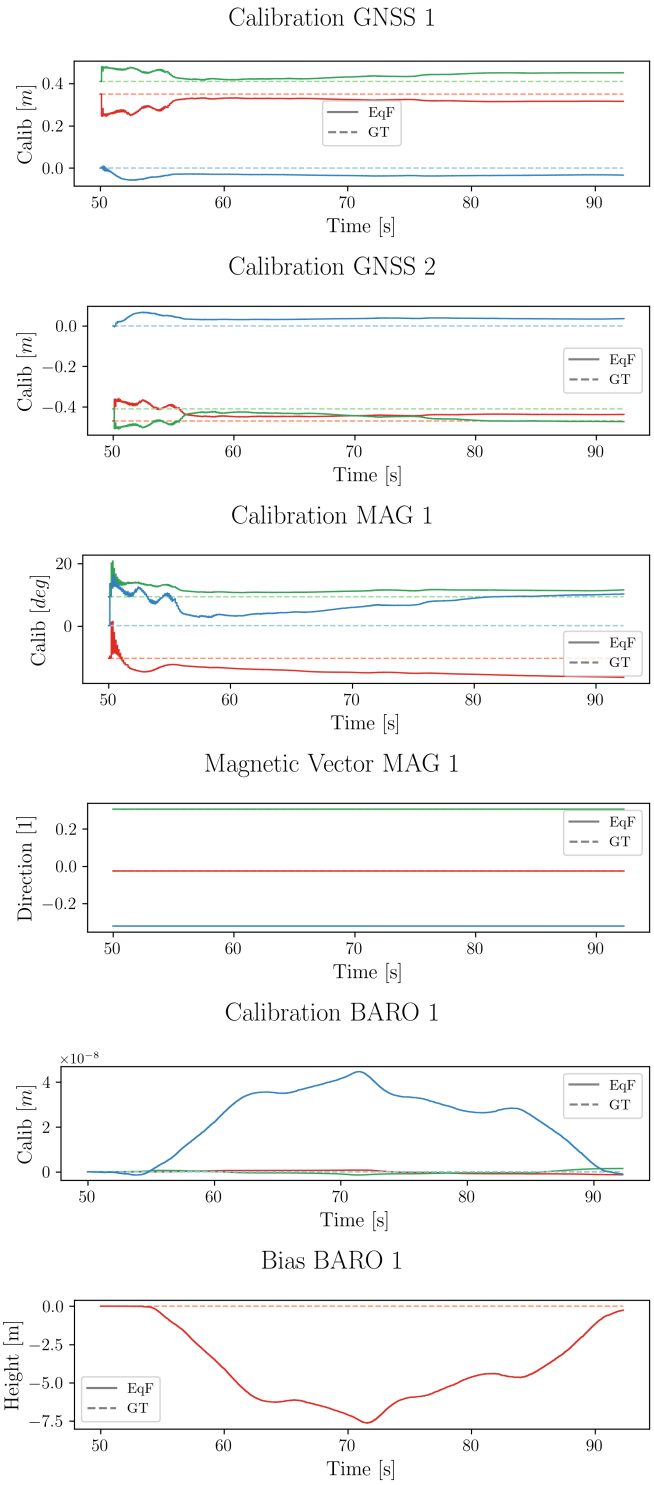

Fig. 2. Auxiliary state estimates of the presented EqF (solid lines) compared to the ground truth values (dashed lines). For the calibration states and magnetic vector the colors red, green, and blue represent the x, y, and z axes, respectively.

REFERENCES

[1] P. van Goor, T. Hamel, and R. Mahony, "Equivariant filter (EqF): A General Filter Design for Systems on Homogeneous Spaces," in *2020 59th IEEE Conference on Decision and Control (CDC)*. Jeju, Korea (South): IEEE, 2020, pp. 5401–5408, arXiv:2107.05193 [eess.SY]. https://ieeexplore.ieee.org/document/9303813

[2] ——, "Equivariant Filter (EqF)," *IEEE Transactions on Automatic Control*, vol. 68, no. 6, pp. 3501–3512, June 2023, arXiv:2010.14666 [eess.SY]. https://ieeexplore.ieee.org/document/9840886/

[3] A. Barrau and S. Bonnabel, "The Invariant Extended Kalman Filter as a Stable Observer," *IEEE Transactions on Automatic Control*, vol. 62, no. 4, pp. 1797–1812, 2017. http://ieeexplore.ieee.org/document/7523335/

[4] A. Fornasier, Y. Ge, P. van Goor, R. Mahony, and S. Weiss, "Equivariant Symmetries for Inertial Navigation Systems," Sept. 2023, arXiv:2309.03765 [cs.RO]. http://arxiv.org/abs/2309.03765

[5] C. Brommer, R. Jung, J. Steinbrener, and S. Weiss, "MaRS: A Modular and Robust Sensor-Fusion Framework," *IEEE Robotics and Automation Letters*, vol. 6, no. 2, pp. 359–366, Apr. 2021. https://ieeexplore.ieee.org/document/9286578/

[6] S. Lynen, M. W. Achtelik, S. Weiss, M. Chli, and R. Siegwart, "A Robust and Modular Multi-Sensor Fusion Approach Applied to MAV Navigation," in *2013 IEEE/RSJ International Conference on Intelligent Robots and Systems*. Tokyo, Japan: IEEE, Nov. 2013, pp. 3923–3929. http://ieeexplore.ieee.org/document/6696917/

[7] X. Ye, F. Song, Z. Zhang, and Q. Zeng, "A Review of Small UAV Navigation System Based on Multisource Sensor Fusion," *IEEE Sensors Journal*, vol. 23, no. 17, pp. 18 926–18 948, Sept. 2023. https://ieeexplore.ieee.org/document/10179240/

[8] A. Barrau and S. Bonnabel, "The Geometry of Navigation Problems," *IEEE Transactions on Automatic Control*, vol. 68, no. 2, pp. 689–704, Feb. 2023, arXiv:2201.04426 [cs, eess]. https://ieeexplore.ieee.org/document/9689974/

[9] T. Zhang, K. Wu, J. Song, S. Huang, and G. Dissanayake, "Convergence and Consistency Analysis for a 3-D Invariant-EKF SLAM," *IEEE Robotics and Automation Letters*, vol. 2, no. 2, pp. 733–740, Apr. 2017. http://ieeexplore.ieee.org/document/7812660/

[10] C. Liu, C. Jiang, and H. Wang, "InGVIO: A Consistent Invariant Filter for Fast and High-Accuracy GNSS-Visual-Inertial Odometry," *IEEE Robotics and Automation Letters*, vol. 8, no. 3, pp. 1850–1857, Mar. 2023, arXiv:2210.15145 [cs.RO]. https://ieeexplore.ieee.org/document/10040716/

[11] A. Fornasier, Y. Ng, R. Mahony, and S. Weiss, "Equivariant Filter Design for Inertial Navigation Systems with Input Measurement Biases," in *2022 International Conference on Robotics and Automation (ICRA)*. Philadelphia, PA, USA: IEEE, 2022, pp. 4333–4339, arXiv:2202.02058 [cs.RO]. https://ieeexplore.ieee.org/document/9811778

[12] M. Scheiber, A. Fornasier, C. Brommer, and S. Weiss, "Revisiting Multi-GNSS Navigation for UAVs – An Equivariant Filtering Approach," in *2023 21st International Conference on Advanced Robotics (ICAR)*. Abu Dhabi, UAE: IEEE, Dec. 2023, pp. 134–141, arXiv:2310.10597 [cs.RO]. https://ieeexplore.ieee.org/document/10406552/

[13] A. Fornasier, Y. Ge, P. van Goor, M. Scheiber, A. Tridgell, R. Mahony, and S. Weiss, "An Equivariant Approach to Robust State Estimation for the ArduPilot Autopilot System," in *2024 IEEE International Conference on Robotics and Automation (ICRA)*. Yokohama, Japan: IEEE, 2024, presented May 2024.

[14] P. van Goor and R. Mahony, "EqVIO: An Equivariant Filter for Visual Inertial Odometry," *IEEE Transactions on Robotics*, vol. 39, no. 5, pp. 3567–3585, 2023, arXiv:2205.01980 [cs.RO]. https://ieeexplore.ieee.org/document/10179117

[15] A. Fornasier, P. Van Goor, E. Allak, R. Mahony, and S. Weiss, "MSCEqF: A Multi State Constraint Equivariant Filter for Vision-Aided Inertial Navigation," *IEEE Robotics and Automation Letters*, vol. 9, no. 1, pp. 731–738, Jan. 2024, arXiv:2311.11649 [cs.RO]. https://ieeexplore.ieee.org/document/10325586/

[16] J. Solà, J. Deray, and D. Atchuthan, "A micro Lie theory for state estimation in robotics," Dec. 2021, arXiv:1812.01537 [cs.RO]. http://arxiv.org/abs/1812.01537

[17] R. Mahony and J. Trumpf, "Equivariant Filter Design for Kinematic Systems on Lie Groups," Aug. 2020, arXiv:2004.00828 [eess.SY]. http://arxiv.org/abs/2004.00828

[18] A. Fornasier, Y. Ng, C. Brommer, C. Böhm, R. Mahony, and S. Weiss, "Overcoming Bias: Equivariant Filter Design for Biased Attitude Estimation With Online Calibration," *IEEE Robotics and Automation Letters*, vol. 7, no. 4, pp. 12 118–12 125, 2022, arXiv:2209.12038 [cs.RO]. https://ieeexplore.ieee.org/document/9905914/

[19] C. Brommer, C. Bohm, J. Steinbrener, R. Brockers, and S. Weiss, "Improved State Estimation in Distorted Magnetic Fields," in *2020 International Conference on Unmanned Aircraft Systems (ICUAS)*. Athens, Greece: IEEE, Sept. 2020, pp. 1007–1013. https://ieeexplore.ieee.org/document/9213913/

[20] C. Brommer, A. Fornasier, M. Scheiber, J. Delaune, R. Brockers, J. Steinbrener, and S. Weiss, "The INSANE dataset: Large number of sensors for challenging UAV flights in Mars analog, outdoor, and out-/indoor transition scenarios," *The International Journal of Robotics Research*, p. 02783649241227245, Feb. 2024, arXiv:2210.09114 [cs.RO]. http://journals.sagepub.com/doi/10.1177/02783649241227245